

Dipole-trap model and non-dispersive charge-carrier transport in polymers of various structures

This article has been downloaded from IOPscience. Please scroll down to see the full text article.

1994 J. Phys.: Condens. Matter 6 10519

(<http://iopscience.iop.org/0953-8984/6/48/013>)

View [the table of contents for this issue](#), or go to the [journal homepage](#) for more

Download details:

IP Address: 171.66.16.179

The article was downloaded on 13/05/2010 at 11:26

Please note that [terms and conditions apply](#).

Dipole-trap model and non-dispersive charge-carrier transport in polymers of various structures

S V Novikov and A V Vannikov

A N Frumkin Institute of Electrochemistry, Russian Academy of Sciences, Leninsky Prospect 31, 117031, Moscow, Russia

Received 8 April 1994

Abstract. We present a development of the dipole-trap model for the description of the field and temperature dependences of the non-dispersive charge-carrier transport in disordered organic matrices. Very good agreement between our numerical results and the phenomenological Gill–Pfister equation is obtained. Our consideration reveals the physical meaning of the parameters of this equation.

1. Introduction

Polymers in which the charge-carrier drift mobility μ can be measured by a straightforward time-of-flight method can be divided into the following groups:

- (i) molecularly doped polymer systems, such as aromatic amines in polyesters;
- (ii) carbon-chain polymers with chromophoric aromatic pendent groups, e.g. poly(*N*-vinylcarbazole) (PVK);
- (iii) polymers with transport sites in the backbone, such as poly(hydroxyaminoester)s [1]; and
- (iv) σ - and π -conjugated polymers, e.g. polysilylenes [2, 3] and poly(*p*-phenylene vinylene)s [4].

In groups (i)–(iii) the localized transport sites are associated with nitrogen atoms conjugated with phenyl groups. In polymers of group (iv) the transport sites are domains like a suborganization of the chain [2] or so-called effectively conjugated segments [4]. The common feature of the non-dispersive charge-carrier transport in the systems listed above is the similar dependences of μ on the electric field F and temperature T , which are described by the empirical equation proposed by Gill [5]:

$$\mu = \mu_0 \exp[-(E_0 - \beta F^{1/2})(T^{-1} - T_0^{-1})] \quad (1)$$

and in slightly different form by Pfister [6]. Here we use a system of units with $k_B = 1$.

The similarity of transport behaviour allowed the suggestion that the same common but incompletely elucidated mechanism of electronic transport by thermal emission from localized states, which has been established for molecularly doped polymers, also operates in π - and σ -conjugated polymers [2]. Equation (1) is often connected with the Poole–Frenkel (PF) effect [7, 8], for two reasons. First, μ depends on F as $\ln \mu \propto F^{1/2}$, as predicted by the PF effect; secondly, the experimental values of coefficient β approximately correspond to the values calculated from the equation for the PF factor:

$$\beta_{PF} = 2(e^3/\epsilon)^{1/2}. \quad (2)$$

Here ϵ is the dielectric constant. Unfortunately, the PF effect can only formally explain the observed field dependence because of the absence of sufficient concentrations of charged traps in the polymer matrices studied.

There are several models of charge transport in disordered organic matrices that do not require the presence of charged traps, as does the PF model, namely small-polaron hopping [9], hopping in a Gaussian density of states (DOS) [10–12] and the Marcus [13] theory of electron transfer, among others. Unfortunately, the Marcus theory and the model of small-polaron hopping cannot explain the field dependence of μ of the type $\ln \mu \propto F^{1/2}$. The model of hopping in a Gaussian DOS does not include any direct molecular parameters of polymer systems. In recent years the Gaussian model has been developed in detail [14–17], and numerous attempts at comparison with experimental results have been made [10, 18–21]. We emphasize the remaining problems and difficulties of the Gaussian model.

(i) A serious problem is the very narrow domain of field F where the dependence $\ln \mu \propto F^{1/2}$ is obeyed [22].

(ii) Non-dispersive transport is experimentally observed under conditions where the Gaussian model predicts a dispersive one, i.e. where $\sigma/T > 4.4$, where σ is the width of the Gaussian distribution [22].

(iii) It is rather difficult to understand the independence of σ on temperature, especially in situations where σ is comparable to T (e.g. $\sigma \simeq (6-7) \times 10^{-2}$ eV and $T \simeq 300$ K [20]).

(iv) In situations where $\sigma/T \gg 1$ (e.g. $\sigma/T = 4-6$), the deep tail of the distribution gives the main contribution to non-dispersive (equilibrium) charge transport. The functional form of the distribution in this asymptotic domain may not be Gaussian at all. An approximate Gaussian form for the DOS in the vicinity of its maximum may be guaranteed by the central-limit theorem, but the tail of the density is commonly formed by rare fluctuations of the environment, so the central-limit theorem cannot be applied here. In a recent paper by Dieckmann *et al* [23] the exact DOS was computed for the cubic lattice with sites occupied by dipoles with random orientation. It was found that, at least for a small dipole concentration, the resulting DOS has totally non-Gaussian form. We intend to consider this crucial problem carefully in a separate paper [24].

(v) To the best of our knowledge, in all cases where experimental data have been compared with theory, the following formula for the mobility has been used:

$$\mu = \mu_0 \exp\{-(2\sigma/3T)^2 + C[(\sigma/T)^2 - \Sigma^2]F^{1/2}\} \quad (3)$$

where Σ is a parameter that characterizes the degree of positional disorder and C is an empirical 'constant' (though dependent on average intersite distance r) given as 2.9×10^{-4} cm^{1/2} V^{-1/2}. Surprisingly, in a recent paper [25] Bässler points out that, instead of F , one must use a dimensionless field $F_{\text{eff}} = eFr/2T$ in equation (3). Consequently, the 'constant' C becomes dependent not only on r , but on the temperature too! Bässler argues that possible corrections are expected to be small. Nevertheless, it would be much better to compare experimental results with the true expression for the mobility, especially because one of the strong arguments in favour of the Gaussian model is close agreement between experimental and theoretical values of C [11, 19, 26, 27].

For these reasons we suggest the simplest transport model in which the main parameter is the dipole moment of the trap (or the transport site) [28, 29].

2. Dipole-trap model: formulation

Suppose that the mobility value is limited by the escape rate of charge carriers from the dipole trap (transport centre) with depth E_0 . For a rough estimation of the effect we suppose

that the main contribution to the escape probability is given by the trajectories that pass through the close vicinity of the saddle point of the potential energy where the activation energy is minimal. Thus we assume that the electric field affects the escape rate mostly by decreasing the activation energy. The saddle-point coordinates depend on the mutual orientation of the field F and the trap dipole moment d . Hence, we produce an averaging over the dipole orientations. In this averaging we consider the influence of the field on the dipole's orientation. The final expression for the mobility has the form [28]:

$$\mu = \mu_0 \int_0^\pi d\alpha \sin \alpha \exp\left(-\frac{E_0 + \delta E_0(\alpha, F) - dF \cos \alpha}{T}\right) \quad (4)$$

where

$$\delta E_0(\alpha, F) = -e(dF^2/\varepsilon)^{1/3} \{3[1/\rho_s^4 - (\cos \alpha)/\rho_s]\}^{1/2}$$

and

$$\rho_s(\alpha) = \left\{\frac{1}{2}[(8 + \cos^2 \alpha)^{1/2} - \cos \alpha]\right\}^{1/3}.$$

Here α is the angle between vectors d and F and $\delta E_0(\alpha, F)$ is the change of trap depth from the case $F = 0$. The distance between the saddle point and dipole is equal to

$$r_s = (d/\varepsilon F)^{1/3} \rho_s(\alpha) \quad (5)$$

and for a typical experimental range of electric field 10^4 – 10^6 V cm⁻¹, $r_s = 10$ – 40 Å. Because of this small value of r_s we believe that, first, we should use $\varepsilon \simeq 1$ – 2 in our formula and, secondly, there is no actual direct relation between the slope of the mobility–field dependence and the macroscopic static dielectric constant of the polymer matrix, which is commonly used in equation (2).

We can make a rough estimation of the slope coefficient of the mobility–field dependence directly from equation (4):

$$\frac{\beta}{T} \simeq \frac{\partial \ln \mu}{\partial F^{1/2}} \propto \frac{e}{T} \left(\frac{d}{\varepsilon}\right)^{1/3} F^{1/6} \quad (6)$$

which for room temperature gives values of about 10^{-3} – 10^{-2} cm^{1/2} V^{-1/2}, in good agreement with experimental data. This estimation depends only very weakly on the matrix and dopant parameters, so we can explain the universality of the coefficient β .

Using this model we can explain the ubiquitous appearance of the field dependence (1) (without the $1/T_0$ term) without needing the assumption of the presence of charged traps in high concentration in polymer matrices. This dependence is intermediate between the low-field region ($F \ll F_t$) and the high-field region ($F \gg F_t$), where the orientation of the dipoles by the electric field F occurs, and $F_t \simeq 0.01e^3/sd^2$. Numerical calculations give the following simple expression for the coefficient β :

$$\beta \simeq 0.36\beta_{PF}. \quad (7)$$

We have tried to describe real experimental data [9] using our formula. These data were chosen because of the extremely broad interval of fields investigated. We obtained very good agreement between the experimental and theoretical field dependences, but the

optimal values of our fitting parameters, the dipole moment d and the dielectric constant ε , were too high: $d \simeq 18$ D and $\varepsilon \simeq 7.5$. We think the reason is that high values of ε and especially of d are needed to move the transition region to the low-field values. In this low-field region our basic assumption about carrier escape in the close vicinity of the saddle point only is not strictly valid owing to the poor separation of the saddle point. In this situation we must consider the charge-carrier dynamics in a trap.

We consider the carrier dynamics using a stochastic approach, assuming that the carrier energy E is the only significant constant of motion. The dynamics of the probability density $P(E, t)$ is governed by a Markovian master equation

$$\frac{\partial P}{\partial t} = \int_{E_{\min}}^{\infty} dE' [K(E, E')P(E', t) - K(E', E)P(E, t)] - k_d(E)P(E, t). \quad (8)$$

Here the kernel $K(E, E')$ is the transition probability for a change in energy from E' to E per unit time, $k_d(E)$ is the decay constant of a bound state of the carrier in a trap, and E_{\min} is the energy of the bottom of a potential well. For classical dynamics $k_d(E) = 0$ for $E < E_{\max}$, where E_{\max} is the decay threshold. The kernel $K(E, E')$ was chosen in the form of the so-called BGK kernel [30]. The physical meaning of the BGK kernel is rather simple: every collision conserves the particle's coordinates and randomizes its momentum according to a Maxwell-Boltzmann distribution. A detailed motivation for this choice may be found elsewhere [29].

Calculation of the escape constant k_e may be carried out in two ways. The first is by direct Monte Carlo simulation of the sequence of the carrier's random jumps in energy, keeping in mind that escape occurs as soon as the carrier reaches an energy above the threshold E_{\max} . Thus, we may express k_e in terms of the average time t_a for the carrier to climb from the bottom of the potential well E_{\min} to the threshold energy E_{\max} :

$$k_e = t_a^{-1}. \quad (9)$$

(In our model the threshold energy E_{\max} is equal to $\delta E_0(\alpha, F)$ from equation (4).) Details of such a calculation were presented in our previous paper [29]. The major disadvantage of this method is its inability to provide the escape rate constant at low temperatures because of an exponential increase in the simulation time.

The second method of calculation of k_e is a straightforward solution of the kinetic equation (8) and calculation of the steady-state probability density $P_s(E, t)$:

$$P_s(E, t) = P_s(E) \exp(-k_e t). \quad (10)$$

The function $P_s(E)$ is the eigenfunction of the integral operator

$$\int_{E_{\min}}^{E_{\max}} dE' K(E, E') P_s(E') = \lambda P_s(E) \quad (11)$$

which corresponds to the largest eigenvalue λ . A non-degeneracy of λ gives us the possibility to compute $P_s(E)$ by iteration

$$\int_{E_{\min}}^{E_{\max}} dE' K(E, E') P_i(E') = P_{i+1}(E) \quad (12)$$

which converges rapidly to $P_s(E)$ for almost any initial function $P_0(E)$. Then we calculate k_e using the equation

$$k_e = \nu_0 - \lambda = \left(\int_{E_{\min}}^{E_{\max}} dE P_s(E) \right)^{-1} \int_{E_{\max}}^{\infty} dE \int_{E_{\min}}^{E_{\max}} dE' K(E, E') P_s(E') \quad (13)$$

which is a consequence of the normalization of the BGK kernel

$$\int_{E_{\min}}^{\infty} dE K(E, E') = \nu_0. \quad (14)$$

The use of equation (13) instead of the direct calculation of λ from equation (11) permits us to avoid the direct subtraction of the exponentially close quantities ν_0 and λ . The computation time t_c of the numerical realization of this method is mostly determined by the calculation of the kernel $K(E, E')$,

$$K(E, E') = \frac{1}{\Omega(E')} \int d\Gamma d\Gamma' \delta(E - H(\Gamma)) \delta(E' - H(\Gamma')) K(\Gamma, \Gamma') \quad (15)$$

via numerical integration. Here $\Omega(E)$ is the density of states,

$$\Omega(E) = \int d\Gamma \delta(E - H(\Gamma)) \quad (16)$$

and $H(\Gamma)$ is the Hamiltonian of the system. The BGK kernel in the phase space $\Gamma = (r, p)$ has the form

$$K(\Gamma, \Gamma') = \nu_0 \delta(r - r') P_{\text{eq}}(p) \quad (17)$$

where ν_0 is the mean frequency of the carrier 'collisions' with the environment, and $P_{\text{eq}}(p)$ is the equilibrium distribution function of the momentum p . The function $K(E, E')$ is computed for the discrete set of its arguments E and E' , and one can expect that the required grid size $\Delta E = E_i - E_{i-1}$ is dictated by the relation $\Delta E \propto T$ (and this was confirmed afterwards). Consequently, we may estimate t_c for this method as

$$t_c \propto T^{-2} \quad (18)$$

while for the Monte Carlo method

$$t_c \propto \exp[(E_{\max} - E_{\min})/T]. \quad (19)$$

Comparison of (18) with (19) shows that this second method has a substantial advantage over the Monte Carlo method for the computation of k_e for deep traps or low temperatures.

The above calculations give us the charge-carrier escape rate at a fixed angle α between vectors F and d . To obtain the mobility μ we must carry out an averaging over the dipole orientations

$$\mu \propto \int_0^\pi d\alpha W(\alpha) k_e(\alpha) \quad (20)$$

where $W(\alpha)$ is the angular distribution function for dipoles. We used two different functions: the first for a fully random dipole orientation, i.e.

$$W(\alpha) = \frac{1}{2} \sin \alpha \quad (21)$$

and the second for a free dipole in the electric field, i.e.

$$W(\alpha) = (dF/2T) \sinh^{-1}(dF/T) \sin \alpha \exp[(dF/T) \cos \alpha]. \quad (22)$$

3. Dipole-trap model: computer simulation results

3.1. Mobility field and temperature dependences

It was shown in our previous paper [29] that the field dependences of the mobility have a typical PF form. The slopes of the linear region on these curves are in good agreement with experimental values. Moreover, the existence of a linear region is a consequence of the carrier dynamics and not the orientation effect, as was the case for the previous rough approximation. Indeed, a linear region is already observed for the field dependence of the escape rate constant at different fixed angles between vectors \mathbf{F} and \mathbf{d} , as seen in figure 1.

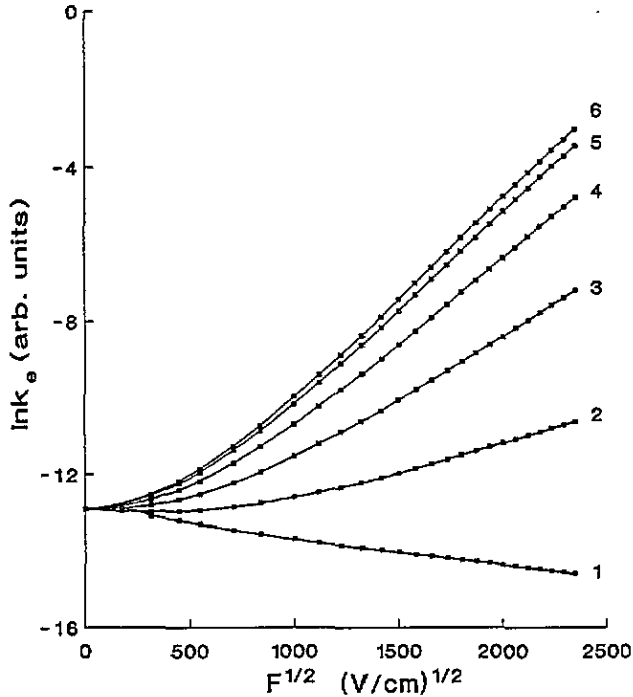


Figure 1. Field dependence of the rate constant k_e at various angles α , which vary from 0 to π with step $\pi/5$ for curves 1–6. Calculations were carried out for $d = 6 D$, $\varepsilon = 2$, $E_0 = 0.8$ eV and $T/E_0 = 0.05$.

We measure the escape rate constant (and, correspondingly, mobility) by the inverse average number of ‘collisions’ with the environment needed to free a charge carrier from the trap. Hence, in our model, the value of k_e cannot be greater than 1, and the equality $k_e = 1$ (or $\mu = 1$) is, in fact, equivalent to instantaneous carrier escape from the trap. To obtain the true escape constant, k_e should be multiplied by ν_0 .

We propose a possible explanation for the deviation of the field dependence of the escape rate constant from the law $\ln k_e \propto F^{2/3}$, which follows from the estimation of k_e from the activation energy decrease. An electric field F affects the charge carrier’s motion in the trap in two ways: first, through the change of activation energy, and, secondly, through the influence on carrier dynamics. In a sufficiently low field, the main influence on the carrier dynamics is provided by the change of the long-range behaviour of the charge-dipole

potential energy, which manifests itself through the restriction of the long-range tail of the potential energy. For a long-range potential energy, a particle with an energy just below the threshold spends most of the time far away from the trap, where its velocity is very small, so the kinetic energy E_k is small too. Hence the distribution function $P(E, E_k)$ for the particle to have a kinetic energy E_k while having total energy E has a sharp maximum at $E_k \rightarrow 0$ provided $E \rightarrow E_{\max}$. The electric field restricts this long-range tail and shifts the maximum in the distribution to greater E_k . The mechanism of the interaction of a charge carrier with the thermal fluctuations that we used includes a resetting of E_k at every 'collision' with the environment, so this shift of the maximum results in an increase of energy dissipation rate just below the threshold and a corresponding decrease of the escape rate constant. This effect most clearly manifests itself in the case $\alpha = 0$ (figure 1), where the activation energy does not depend on F ($\delta E_0(0, F) = 0$), and the aforementioned first factor does not exist. In this case the second factor's influence leads to the decrease of μ with increase of F . For not so small values of angle α , a change of activation energy dominates over this effect, but, nevertheless, it still weakens the escape rate-field dependence.

Numerical results obtained at very low temperature show a much closer correlation of the mobility-field dependence, obtained for the random dipole distribution (21), with the relation $\ln \mu \propto F^{2/3}$ (figure 2). So part of the deviation of the mobility-field dependence at high temperature from the 'genuine' dipole behaviour may be associated with the peculiar kind of 'repulsion' of the mobility-field curve from the limiting value $\mu_{\max} = 1$. More strictly, in the vicinity of μ_{\max} the rate of the mobility increase with field (or temperature) is slowing down, which leads to the change of the mobility-field (or mobility-temperature) dependences. For the mobility-field dependences it leads to a change from the $\ln \mu \propto F^{2/3}$ dependence to one more like $\ln \mu \propto F^{1/2}$.

Our previous results were based on the Monte Carlo simulation only. We have found that the overall mobility-field and mobility-temperature dependences for moderately strong fields are described sufficiently well by the formula

$$\mu = \mu_0 \exp[-\beta(F_0^{1/2} - F^{1/2})(T^{-2} - T_0^{-2})]. \quad (23)$$

A totally non-Arrhenius temperature dependence is very unusual for the escape rate constant. The only way of verifying it is to perform calculations of k_e over a wider temperature range (i.e., in our case, for lower temperatures). Now we are able to carry out such a calculation using computation of the steady-state probability density. Results of this calculation are shown on figure 3. We can state that the mobility-temperature dependence has a complicated form, being an Arrhenius one at low temperatures and significantly deviating from this with increase of temperature. A strong argument in favour of the Arrhenius type of temperature dependence at low temperature is the close agreement between the curve's slope and corresponding trap depth. At high temperature this dependence closely resembles a $\ln \mu \propto 1/T^2$ dependence. This weakening of the mobility-temperature dependence is another manifestation of the slowing down of the mobility increase in the vicinity of the limiting value $\mu \simeq 1$. Experimental data on the mobility-temperature dependence may be approximated either by a $\ln \mu \propto 1/T$ dependence or by a $\ln \mu \propto 1/T^2$ dependence according to the temperature range investigated. A comprehensive analysis of the advantages of using a $\ln \mu \propto 1/T$ or $\ln \mu \propto 1/T^2$ dependence for the description of the experimental data may be found in reviews [22, 25]. For low temperatures, the overall field and temperature dependences of the mobility are in very good agreement with the Gill-Pfister equation (1) (see figures 3 and 4). Our preliminary calculations show that intersection of the Arrhenius curves plotted for the different field values is probably a common phenomenon: it is

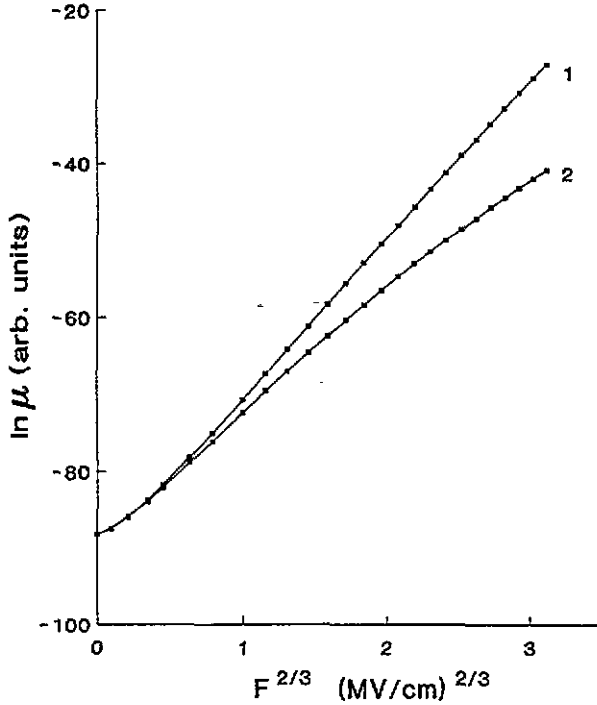


Figure 2. Plot of $\ln \mu$ versus $F^{2/3}$ at very low temperature. Curve 1 was obtained for the random dipole distribution (21) and curve 2 for the distribution (22). Parameter values: $E_0 = 0.8$ eV, $T/E_0 = 0.01$, $d = 6$ D and $\epsilon = 2$.

observed for such different types of potential energy as Coulomb and Gaussian, too. A detailed discussion of this phenomenon will be published in a separate paper. Nevertheless, we may reasonably assume that the insensitivity of the phenomenon to the form of the potential energy implies that the only essential parameter that determines the value of T_0 is the trap depth E_0 : $T_0 \propto E_0$. One can see on figure 3 that

$$T_0 \approx 0.1E_0. \quad (24)$$

Moreover, the coefficient of proportionality in equation (24) is also approximately insensitive to the form of the potential energy. Such robustness of the intersection phenomenon raises important questions about its nature, in particular about its relation to the mechanism of thermal activation of a carrier (BGK mechanism). Relation (24), albeit very crude, is approximately verified by a vast collection of experimental data [31–35].

In most papers the phenomenological temperature T_0 from the Gill–Pfister equation (1) is directly interpreted as the temperature of the real inversion of the sign of the mobility–field dependence slope. The dipole-trap model, with BGK mechanism of thermal activation, cannot describe such behaviour. It is of interest to note that while equation (1) describes a great variety of experimental data, direct observation of real inversion is an extremely rare phenomenon. Usually the temperature T_0 is far greater than the glass transition temperature of the polymer matrix. These observations and the results of our simulation suggest that, for most systems, the temperature T_0 is, probably, not a temperature of real inversion at all. It is possible that a real inversion of the sign of the slope of the mobility–field dependence

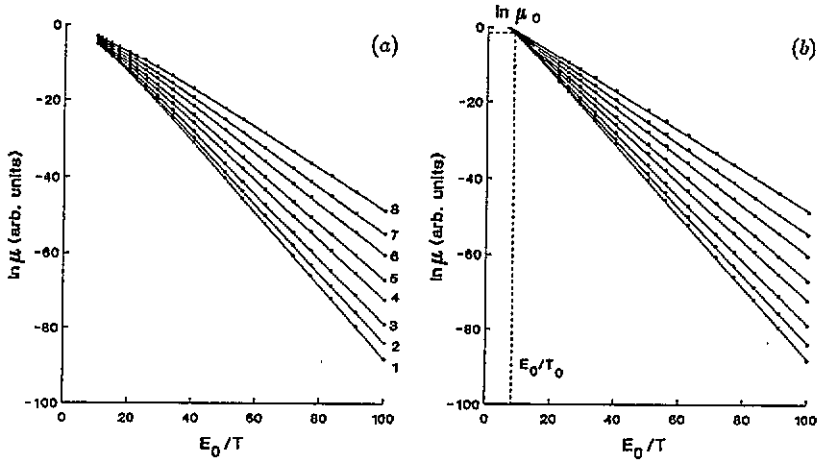


Figure 3. (a) Temperature dependence of the mobility at various electric fields, which have the following values for curves 1–8, respectively: 0, 2, 5, 10, 15, 22.5, 30 and $40 \times 10^5 \text{ V cm}^{-1}$. All other parameters have the same values as in figure 2, and the averaging (22) is used. (b) Here we draw straight lines to fit points obtained only for temperatures less than $0.05 E_0$.

is not a general feature of the charge-carrier transport in disordered organic matrices, but rather a special case resulting from the action of some particular mechanism.

Also we wish to emphasize the particular mobility value μ_0 (to be precise, k_e), which corresponds to the intersection point. In our model

$$\mu_0 \simeq 1 \quad (25)$$

and approximately agrees with the maximal possible mobility μ_{\max} (i.e. mobility at $T \rightarrow \infty$, which is independent of F). Hence, in our model the real carrier mobility at $T \rightarrow \infty$ is μ_0 , and not $\mu_0 \exp[(E_0 - \beta F^{1/2})/T_0]$, as follows formally from equation (1) (see also figure 3). Some years ago Borsenberger [36] noted that extrapolation to $T = \infty$ at $F = 0$ according to an Arrhenius temperature dependence gives an unreasonably high mobility, while extrapolation according to a $\ln \mu \propto 1/T^2$ dependence gives a reasonable one (in his particular case, $10^4 \text{ cm}^2 \text{ V}^{-1} \text{ s}^{-1}$ and $0.19 \text{ cm}^2 \text{ V}^{-1} \text{ s}^{-1}$, respectively). Borsenberger emphasized that this distinction is a strong argument in favour of the latter dependence. In our model, extrapolation to $T = \infty$ does not give the real mobility at high temperature, but a value enhanced by the factor

$$\exp(E_0/T_0) \simeq e^{10} \simeq 2 \times 10^4. \quad (26)$$

So the real high-temperature mobility according to Borsenberger's data should not be $10^4 \text{ cm}^2 \text{ V}^{-1} \text{ s}^{-1}$, but about $0.5 \text{ cm}^2 \text{ V}^{-1} \text{ s}^{-1}$, a very reasonable value. The enhancement factor (26) may vary widely because the relation (24) is very approximate, but, nevertheless, we can state with assurance that a simple Arrhenius extrapolation overestimates the mobility value at high temperatures by several orders of magnitude.

Unfortunately, limitation of our computer does not permit us to perform a strict optimization procedure on the fitting of our curves to the Schein *et al* [9] data and to provide a direct comparison with our previous results [28]. Nevertheless, the dynamic effects move the linear region on the $\ln \mu(F^{1/2})$ curves to lower fields, and reduce the

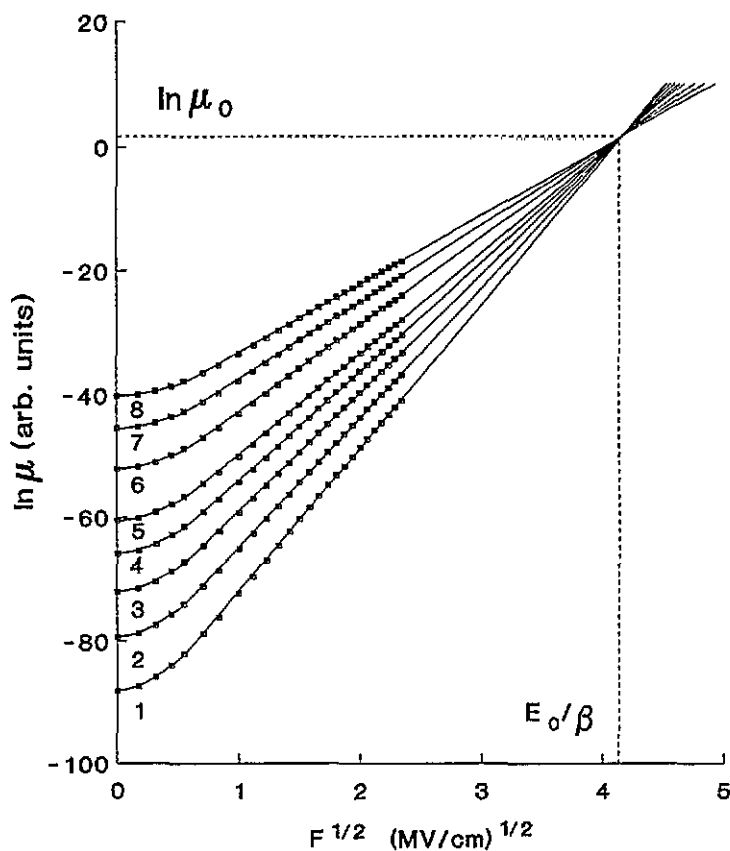


Figure 4. Field dependence of the mobility at various temperatures. The ratio T/E_0 takes the following values for curves 1–8, respectively: 0.010, 0.011, 0.012, 0.013, 0.014, 0.016, 0.018 and 0.020. All other parameters have the same values as in figure 2, and the averaging (22) is used.

slope, so we may anticipate that unusually high d and ε values are not necessary to describe the experimental data. To support this statement we demonstrate in figure 5 the result of a 'poor man's' optimization (optimization by eye) for the fitting of these data. A theoretical curve with $d = 6D$ and $\varepsilon = 2.5$ fits the data very well at $F \geq 4 \times 10^5 \text{ V cm}^{-1}$, but a significant deviation in the low-field region is observed. For comparison we provide the mobility–field dependence calculated with the use of equation (4). Note that the slope of the latter dependence is significantly greater. In fact, according to equation (7), using the orientation effect only, it is impossible to obtain the experimentally observed slope for the mobility–field dependence using reasonable values of ε .

3.2. Zero-field limit

According to our calculations, the mobility–field dependence $\ln \mu(F^{1/2})$ has a distinct curvature in the low-field region, so the real mobility value at zero field differs noticeably from the corresponding value obtained by extrapolation of the curve's linear region to zero field. In recent papers [38, 39] the extrapolated mobility value μ_h^0 was compared with the hole diffusion coefficient D_h via the Einstein equation

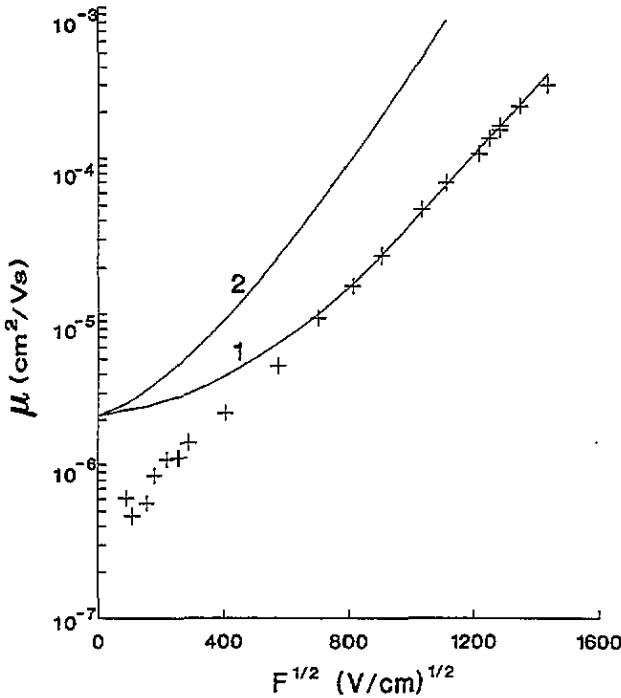


Figure 5. Result of the approximate optimization of the mobility-field dependence for fitting data of Schein *et al* [9]: $d_{\text{opt}} = 6 D$ and $\varepsilon_{\text{opt}} = 2.5$. The escape constant was obtained using computation of the steady-state probability density (11), and the averaging (22) was used (curve 1). For the parameter E_0 we used the experimental value of 0.6 eV [37]. For comparison, we provide the mobility-field dependence calculated with the use of equation (4) (curve 2) for the same values of d and ε .

$$\mu_h^0 = eD_h/T \quad (27)$$

for the model polymer poly(tetraphenylbenzidine) (PTPB). The diffusion coefficient was measured by a standard electrochemical technique both for the polymer layer saturated with liquid electrolyte ('plastified' polymer layer) and for the semi-oxidized PTPB containing the equivalent quantity of counter-ions but without the liquid electrolyte ('solid' polymer layer). It was found that, for the 'solid' layer, equation (27) is obeyed well, while, not surprisingly, for the 'plastified' layer, significant discrepancies were found. The authors argue that agreement between values of μ_h^0 and D_h for the case of the 'solid' layer is a convincing argument for the continuation of the PF-type relation $\ln \mu \propto F^{1/2}$ down to the close vicinity of zero field. This result is in clear disagreement with our model. We think that it is rather risky to reach such a profound conclusion from the aforementioned data as the 'solid' layer differs significantly from samples used in the time-of-flight measurements. Strictly speaking, our model in its present state cannot describe charge transport in very weak fields (about 10^4 V cm^{-1} and less), because the distance between the saddle point and the transport site becomes equal to or exceeds the average distance between the transport sites. In this situation charge transport must be described using multicentre models. Nevertheless, from our point of view, PF-type behaviour in weak fields is very improbable.

4. Conclusions

In recent years much effort has been directed towards describing the main features of the charge transport in polymeric disordered solids. Nevertheless, so far no model has been found that could fully explain the electric field and temperature dependences of the charge-carrier drift mobility in these systems. A possible reason is that various mechanisms of electronic transport apply in different systems and also in different regimes of temperature and electric field, so no single mechanism can be expected to explain the whole variety of the experimental data. Meanwhile there is the well known phenomenological equation (1) suggested by Gill [5] and Pfister [6], which describes well the experimental dependences and correctly predicts the behaviour of these systems at characteristic temperature T_0 and field F_0 . In the present paper the experimentally observed field and temperature dependences of the drift mobility are well explained using the dipole-trap model, which takes into account the charge-carrier dynamics in a trap. The Gill-Pfister equation is a natural result of the dipole-trap model. The main molecular parameter used in the model is the dipole moment of a trap.

At the present state of our knowledge we may explain the ubiquitous appearance of the PF field dependence by using the following arguments. First of all, the ultimate reason for the observation of the PF field dependence is the proximity of the field dependence of the dipole-related change of activation energy $\delta E_0 \propto F^{2/3}$ to the PF dependence. Furthermore, there are some factors that cause additional weakening of the mobility-field dependence and bring it closer to the PF dependence. These factors are:

- (i) the dynamic effect of the restriction of the long-range tail of the potential energy by the external electric field;
- (ii) orientation of the dipoles by the external electric field; and
- (iii) slowing down of the mobility increase in the vicinity of the limiting value μ_0 , which weakens the mobility-field (and mobility-temperature) dependences for relatively shallow traps (e.g. $E_0 \simeq 0.4$ eV at room temperature).

The other important statements of the dipole-trap model are as follows:

- (i) There is no direct relation between macroscopic static dielectric constant ϵ and the mobility-field dependence.
- (ii) The mobility-temperature dependence has a complicated form, being close to Arrhenius at low temperature and resembling the dependence $\ln \mu \propto 1/T^2$ at high temperatures.
- (iii) The characteristic temperature T_0 from the Gill-Pfister equation (1) has a simple approximate relation to the activation energy E_0 : $T_0 \simeq 0.1E_0$.
- (iv) The temperature T_0 for most systems is not a temperature of real inversion of the sign of the slope of the mobility-field dependence.
- (v) A formal extrapolation of the Arrhenius temperature dependence to $T \rightarrow \infty$ overestimates the high-temperature mobility by several orders of magnitude. In terms of the Gill-Pfister equation (1), the real zero-field mobility at high temperature is not $\mu_0 \exp(E_0/T_0)$, but μ_0 .

Obviously, our model in its current form cannot explain some experimentally observed phenomena, such as the change of sign of β at high temperatures, and cannot even pretend to describe dispersive transport (concentration dependences we consider in separate papers [40, 41]). Nevertheless, we hope that this treatment clearly demonstrates the potential usefulness of the model.

Acknowledgments

We are grateful for the support provided by the Russian Foundation for Fundamental Research (Grant No 93-03-5703) and Alfred Sloan Foundation (grant awarded by the American Physical Society).

References

- [1] Vannikov A V and Kryukov A Yu 1990 *J. Inf. Rec. Mater.* **18** 341
- [2] Stolka M and Abkowitz M A 1991 *Synth. Met.* **41–43** 3385
- [3] Abkowitz M A 1992 *Phil. Mag.* **B 65** 817
- [4] Kryukov A Yu, Saidov A Ch and Vannikov A V 1992 *Thin Solid Films* **209** 84
- [5] Gill W G 1972 *J. Appl. Phys.* **43** 5033
- [6] Pfister G 1977 *Phys. Rev. B* **16** 3676
- [7] Poole H H 1916 *Phil. Mag.* **32** 112
- [8] Frenkel J 1938 *Phys. Rev.* **54** 647
- [9] Schein L B, Peled A and Glatz D 1989 *J. Appl. Phys.* **66** 686
- [10] Bässler H 1981 *Phys. Status Solidi b* **107** 9
- [11] Bässler H 1984 *Phil. Mag.* **50** 347
- [12] Borsenberger P M, Pautmeier L and Bässler H 1991 *J. Chem. Phys.* **94** 5547
- [13] Marcus R A 1964 *Ann. Rev. Phys. Chem.* **15** 155
- [14] Pautmeier L, Richert R and Bässler H 1989 *Phil. Mag. Lett.* **59** 325
- [15] Pautmeier L, Richert R and Bässler H 1990 *Synth. Met.* **37** 271
- [16] Pautmeier L, Richert R and Bässler H 1991 *Phil. Mag.* **B 63** 587
- [17] Richert R, Pautmeier L and Bässler H 1989 *Phys. Rev. Lett.* **63** 547
- [18] Borsenberger P M 1992 *Polym. Prepr.* **33** 806
- [19] Borsenberger P M, Pautmeier L and Bässler H 1991 *J. Chem. Phys.* **95** 1258
- [20] Borsenberger P M and Bässler H 1992 *Phys. Status Solidi b* **170** 291
- [21] Borsenberger P M and Rossi L J 1992 *J. Chem. Phys.* **96** 2390
- [22] Schein L B 1992 *Phil. Mag.* **B 65** 795
- [23] Dieckmann A, Bässler H and Borsenberger P M 1993 *J. Chem. Phys.* **99** 8136
- [24] Novikov S V and Vannikov A V 1994 *Phys. Lett. A* submitted
- [25] Bässler H 1993 *Phys. Status Solidi b* **175** 15
- [26] Borsenberger P M and Fitzgerald J J 1993 *J. Phys. Chem.* **97** 4815
- [27] Borsenberger P M, Magin E H, van der Auweraer M and de Schryver F C 1993 *Phys. Status Solidi a* **140** 9
- [28] Novikov S V and Vannikov A V 1991 *Chem. Phys. Lett.* **182** 598
- [29] Novikov S V and Vannikov A V 1993 *Chem. Phys.* **169** 21
- [30] Bhatnagar P L, Gross E P and Krook M 1954 *Phys. Rev.* **94** 511
- [31] Stolka M, Abkowitz M A, Knier F E, Weagley R J and McGrane K M 1990 *Synth. Met.* **37** 295
- [32] Yamaguchi Y and Yokoyama M 1991 *J. Appl. Phys.* **70** 3726
- [33] Kitamura T and Yokoyama M 1991 *J. Appl. Phys.* **69** 821
- [34] Sasakawa T, Ikeda T and Tazuke S 1989 *Macromolecules* **22** 4253
- [35] Ulanski J, Sielski J, Glatzhofer D T and Kryszewski M 1990 *J. Phys. D: Appl. Phys.* **23** 75
- [36] Borsenberger P M 1990 *J. Appl. Phys.* **68** 5682
- [37] Schein L B and Mack J X 1988 *Chem. Phys. Lett.* **149** 109
- [38] Facci J S, Abkowitz M, Limburg W, Yanus J and Renfer D 1991 *J. Phys. Chem.* **95** 7908
- [39] Abkowitz M A, Facci J S, Limburg W W and Yanus J F 1992 *Phys. Rev. B* **46** 6705
- [40] Novikov S V and Vannikov A V 1994 *Chem. Phys. Lett.* **224** 501
- [41] Novikov S V and Vannikov A V 1994 *Chem. Phys.* **187** to be published